

HIGH PERFORMANCE FIBROUS BONDED CONCRETE OVERLAYS FOR FULL-DEPTH PRECAST CONCRETE BRIDGE DECK CONSTRUCTION

Mohsen A. Issa, PhD, PE, SE, FACI, Department of Civil and Materials Engineering,
University of Illinois at Chicago (UIC), Chicago, IL

Mohammad A. Alhassan, PhD student, Department of Civil and Materials Eng., UIC

Rajai Z. Alrousan, PhD student, Department of Civil and Materials Eng., UIC

ABSTRACT

Segmental construction of prefabricated full-depth concrete bridge deck systems results in numerous transverse and longitudinal joints as well as shear connector pockets that receive cast-in-place concrete or grout. In such systems, it is necessary to overlay the bridge deck to provide smooth riding surface and to protect the underlying deck reinforcement from the deicing salts-induced corrosion and consequent spalling and delamination of the concrete.

This paper reports on results and findings obtained from a non-linear finite element analysis (FEA) of a prototype prefabricated full-depth precast concrete bridge deck panel system before and after being overlaid with various plain and fibrous latex-modified concrete (LMC) and microsilica concrete (MSC) overlays. The FEA were validated with experimental results obtained from full-scale testing of the prototype bridge system. The benefits of the FEA can be highly appreciated when visualizing the substantial time and cost savings, the ability to change any parameter of interest, and the capability of demonstrating any interesting response at any load value and at any location in the system. The most attractive results were: (1) Adequately bonded LMC or MSC overlay significantly improves the stiffness, cracking load, and ultimate strength capacity of the system, (2) AASHTO HS20 truck induced bond stresses were below the bond strength of bonded LMC and MSC overlays, (3) The fibrous overlay has desirable crack arresting characteristic.

Keywords: Overlay, bridge decks, Segmental construction, Latex-modified concrete, LMC, Microsilica concrete, MSC, Finite element analysis, Bond strength, AASHTO truck loading.

INTRODUCTION AND BACKGROUND INFORMATION

The prefabricated full-depth precast concrete bridge deck system is a very effective and economic design concept for rehabilitation of existing highway bridges as well as for new bridge constructions. The system is typically composed of high performance prefabricated full-depth precast, post-tensioned concrete panels, high strength longitudinal post-tensioning strands and/or bar systems typically run between the precast concrete deck panels through the joints, shear stud connectors aligned inside shear pockets, and transverse joints¹⁻¹⁰. In stage construction, longitudinal joints along with transverse post-tensioning will be required. The full-depth concrete panels can be either precast or precast/prestressed in the transverse direction depending on the bridge width and/or the type of staged construction involved. Full composite action between the deck and the supporting system (either steel stringers or concrete girders) is achieved by means of shear stud connectors aligned appropriately inside shear pockets. The transverse and longitudinal joints as well as the shear pockets are the only components that receive cast-in-place concrete or grout. In such systems, application of protective overlay is necessary in order to provide smooth riding surface, to protect the underlying concrete deck from deterioration, and more importantly to protect the steel reinforcement and the post-tensioning strand/bar systems from the deicing salts-induced corrosion.

Typically, segmental bridges are designed to last more than 75 years, while the typical target service life of a concrete overlay ranges from 20 to 25 years under the exposure to the application of deicing chemicals and thermal movements as well as fatigue live loading. In terms of cost, time, and effort, replacing the overlay every 20-25 years after becoming contaminated with deicing salts and functionally-obsolete is much more economical than replacing or repairing the bridge deck system. Moreover, the overlay will keep the underlying precast concrete deck system in a high quality condition. Protective overlays that include Latex Modified Concrete (LMC), Micro Silica Concrete (MSC), and epoxy overlays are being employed as corrosion protection strategies on bridge decks. The overlay must be free of severe cracking to fulfill its intended functionality. The bond between the overlay and the bridge deck is the key factor that insures such functionality. Once the overlay is debonded, it will be severely cracked and delaminated within a short period of time under the aggressive environmental exposures and fatigue live loadings and impact¹⁰. Successful application of an overlay can be accomplished through the use of well-proportioned overlay mixtures along with acceptable construction practices in terms of the deck surface preparation, mixing, casting, finishing, and curing. Unfortunately, most of the previous and recent overlay projects were experienced severe deterioration after less than 10 years and in many cases within 1 to 3 years as a result of poor construction practices and inappropriate mixture design proportioning¹¹⁻¹³. In order to have a durable overlay-deck system, the overlay must be sufficiently bonded to the base concrete, resistant to cracking, and have low permeability to prevent chloride ion penetration and the associated corrosion of the deck reinforcement.

This paper reports on results and findings obtained from non-linear finite element analysis (FEA) of a prototype prefabricated full-depth precast concrete bridge deck panel system

before and after being overlaid with various plain and fibrous LMC and MSC overlays. The FEA results were compared with experimental results obtained from full-scale testing of the prototype bridge system. Good agreement between the FEA and the full scale testing was noticed. After validation with the experimental test results, the FEA was used to generate and clarify a number of critical parameters of interest that were difficult to determine by the full-scale testing knowing that the actual LMC and MSC overlays were installed on about 2/3 of the prototype bridge deck surface area. Using material properties almost similar to the LMC and MSC materials with full bond strength (as confirmed by the experimental direct tensile bond strength tests), the behavior of the prototype bridge system with the overlay on the whole deck surface area was obtained. In addition, the results were obtained for the overlaid system with cracked and uncracked bridge deck. Moreover, the state of stresses at the interface between the deck and the overlay was continuously demonstrated versus the applied load. These capabilities of the FEA are highly appreciated especially when the savings of the time and cost are also visualized. Detailed description of the FEA methodology is presented in the subsequent sections.

SIGNIFICANCE OF THE STUDY

Protective overlays with high performance and bond characteristics are essential and provide substantial benefits for segmental bridge deck panel systems. Nonlinear FEA was carried out to model a prototype full-depth precast concrete deck panel system and to simulate its structural response with and without concrete overlay. The FEA results were validated with experimental results and observations obtained from two pioneering projects related to the full-depth system and different plain and fibrous LMC and MSC overlay types. The effectiveness and the power of the FEA into considering and demonstrating various parameters of interest in minimal time and cost were enlightened.

BRIEF DESCRIPTIONS

PROTOTYPE BRIDGE COMPONENTS

A full-scale prototype bridge system (Fig. 1) was designed and built to evaluate its constructability and structural behavior. The prototype bridge system is 18 ft (5.5 m) wide and 82 ft (25 m) long having two equal span lengths of 40 ft (12.2 m) each and composed of 11 prefabricated full-depth precast, post-tensioned concrete panels installed on three W18x86 steel stringers. The segmental deck panels were made fully composite with the supporting stringers using shear stud connectors designed according to AASHTO Standard Specifications¹⁴ and AASHTO LRFD Specifications¹⁵ and aligned inside beveled shear pockets; three rows spaced at 2 ft (610 mm) center to center. The precast concrete panels were 18 ft (5.5 m) wide (full width) and 8 in. (200 mm) in depth designed for transverse flexure with conventional mild reinforcement according in accordance with the current AASHTO deck design provisions^{14,15} for a slab design with the main reinforcement perpendicular to traffic. The two identical end panels were 4 ft-9.5 in. (1.46 m) long, while

the nine middle panels were 8 ft (2.44 m) long and have different end configurations due to the post-tensioning requirements and sequence of construction. This arrangement of the panels was designed to avoid location of a transverse joint directly over the central support. The transverse joints between the adjacent panels were of female-to-female type and received non-shrink cementitious grout. Leveling screws were used to adjust the panels over the supporting system to provide a minimum haunch of 1 in. (25 mm).



Fig. 1 Overall view of the full-scale two-span, two-lane, continuous prototype bridge

The precast concrete panels were cast in the precast yard of Illinois Concrete Co., Inc., Champaign, Illinois. The 28-day compressive strength of the panels was 7100 psi (50 MPa). After 60 days, the panels were delivered to the Illinois Department of Transportation (IDOT) Biesterfield yard, Elk Grove Village, Illinois, to be installed on the prototype bridge system. Longitudinal post-tensioning strand and bar systems were used to provide continuity between the panels. The post-tensioning systems were placed at the mid-height of the panels to provide a uniform stress distribution across the depth. The average post-tensioning stress levels at the central support and at 0.4 L (from each span) were about 500 psi (3.4 MPa) and 330 psi (2.3 MPa), respectively. Detailed information and demonstration figures of the system components, fabrication of the system, the post-tensioning sequence, the transverse joints, the shear pockets and shear stud connectors, and the concrete and grout materials properties are well-documented in several publications²⁻¹⁰.

INSTALLATION OF THE OVERLAYS

Two LMC overlays (LMC plain and LMC with synthetic fibers), three MSC overlays (MSC plain, MSC with steel fibers, and MSC with synthetic fibers), and two epoxy overlays (one

$\frac{3}{8}$ - $\frac{1}{2}$ in. (9-12 mm) thick and one $\frac{1}{4}$ - $\frac{1}{2}$ in. (6-12 mm) thick) were installed on the prototype bridge deck panel system according to the layout shown in Fig. 2.

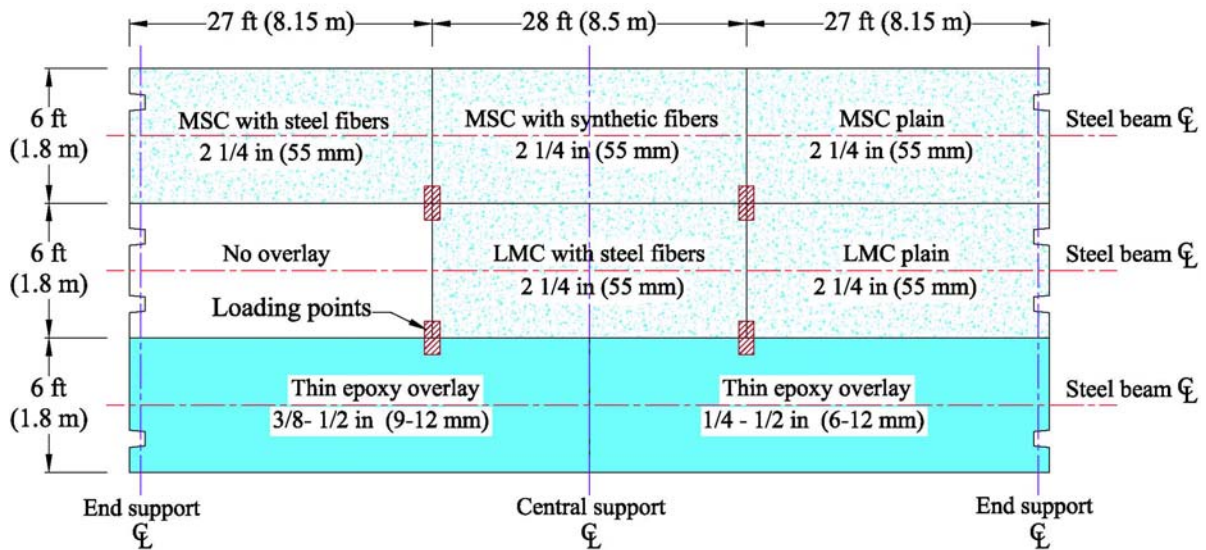


Fig. 2 Layout of the overlays on the prototype bridge system

The main objective was to evaluate the performance of the various overlay types under actual environmental conditions and simulated fatigue loading. The deck surface was prepared using water-jet blasting applying a pressure of about 17,000 to 19,000 psi (115 to 130 MPa) to have the coarse aggregates with a clean exposed surface without being damaged (Fig. 3). Final touch-ups around the corners, edges, and non well-prepared areas, were implemented using sandblasting machines. The deck surface was wetted for 24 hours before receiving the 2 $\frac{1}{4}$ in.- (55 mm) thick LMC and MSC overlays. Compressed air was used to remove any standing water in depressions or holes in the bridge deck, and the surface was kept clean from all foreign materials such as oil, dirt, and dust. The 28-day compressive strengths of the entire LMC and MSC overlay types were approximately 6500 psi (50 MPa).



Fig. 3 Deck surface preparation using water jet blasting

The three MSC overlay mixtures were mixed using ready mix-concrete mixers, while a mobile mixer was used to cast the LMC overlays. All of the LMC and MSC overlay mixtures were discharged to the casting area using a concrete conveyor truck. Fig. 4 shows the ready-mix concrete truck, the mobile mixer, and the conveyor truck. In the fibrous LMC and MSC overlay mixtures; the fibers were premixed with the coarse aggregates. LMC overlay with synthetic fibers was not installed since the rate of discharging process of the premixed synthetic fibers and coarse aggregates from the mobile mixer was not consistent. The LMC and MSC overlays were promptly covered with clean wet burlap as soon as the surface was able to support the burlap. In addition, a polyethylene film was applied on the top of the burlap and held down at the edges. This wet curing continued two days for the LMC overlays and seven days for MSC overlays. Fig. 5 shows portion of the casting, finishing, and curing procedures.



Fig. 4 Portion of the construction practices of the LMC and MSC overlays



Fig. 5 Portion of the casting, finishing, and curing procedures

FULL-SCALE TESTING

The prototype bridge without the overlays was tested for the maximum negative and positive moment cases simulating AASHTO HS20 truck service load along with 30% impact,

overload (2 times the service load), and about 8 times the service load. Then after one year from the installation of the overlays, where the overlays went under one full winter cycle included several freezing and thawing cycles (Fig. 6), the overlaid system was tested again statically before and after applying 300 low fatigue loading cycles for the maximum negative moment service load along with 30% impact, overload, and about 5 times the service load. The reason for applying only about 5 times the service load was to avoid damaging the prototype system destructively since other tests with different parameters will be conducted on the system.



Fig. 6 Accumulation of snow and ice on the prototype bridge deck overlays

A testing bed, 22 ft (6.7 m) wide and 100 ft (30.5 m) long, was designed and fabricated to accommodate the prototype bridge. A total of four very rigid very stiff self-sustained loading frames, each composed of four HP14x89 columns and two W24x94 beams, were designed and fabricated to simulate the effect of AASHTO truck loading. Two frames were used to apply the maximum positive moment case in the first span, while the other two frames were used to apply the maximum negative moment case over the interior central support. Two hydraulic cylinders connected to an electrical hydraulic pump of a capacity of 10,000 psi (70 MPa) were used to load the bridge in small increments. The AASHTO HS20 truck loading was simulated by an equivalent two-axle vehicle loading, 6 ft (1.83 m) wide with a distance of 17 ft (5.18 m) between the two axles. Fig. 7 shows the loading frames and the spread beams. Steel plates of 8 x 20 x 2 in. (200 x 510 x 50 mm) were used to transfer the load from the spread beams to the bridge deck system. Rubber pads were used between the steel plates and the deck system to ensure an even distribution of pressure on the contact areas. A special automatic controlled hydraulic system was designed to apply the low fatigue loading cycles. The stringers as well as the bridge deck system were instrumented with electrical and vibrating wire strain gages as well as linear variable displacement transducers (LVDTs) to obtain the strain and deflection values at the critical locations.



Fig. 7 Loading frames and spread beams

FINITE ELEMENT MODELING METHODOLOGY

The prototype bridge system with and without overlay was modeled using the non-linear finite element ANSYS software, version 9¹⁷, in order to accomplish various benefits after validating the modeling with the full-scale test results. The main benefits that can be obtained from the FEA are: (1) provides substantial savings in the cost, time, and effort, (2) allows to change any parameter of interest to evaluate its influence on the system, such as the post-tensioning level, (3) allows to see the stress, strain, and deflection values at any location and at any load level, (4) allows to evaluate the induced bond stresses versus the applied load value, and (5) supports the experimental test results.

ELEMENTS TYPES

The eight-node element SOLID65 was used to model the bridge deck and the overlay concretes. This solid element is typically used for the 3-D modeling of solids with or without reinforcing bars. The most important aspects of this element are the treatment of the nonlinear material properties and the capability of cracking in the three orthogonal directions, crushing, plastic deformation, and creep. The element LINK10 was used to model the post-tensioning bars and steel studs. LINK10 has unique feature of a bilinear stiffness matrix resulting in a uniaxial tension-only or compression-only. The steel reinforcement was modeled by a LINK8 element, which is a 3-D spar uniaxial tension-compression element. The element is also capable of plastic deformation. The eight-node SOLID45 element was used for the steel beams and the supporting and loading steel plates. All of the used elements have 3 degrees of freedom at each node, translations in the nodal x, y, and z directions.

MATERIALS PROPERTIES

The materials properties used in the experimental testing were employed in the FEA. The concrete properties included a compressive strength and an elastic modulus (E) of 7100 psi

(50 MPa) and 5100 ksi (35 GPa), respectively for the precast concrete deck panels, 5000 psi (35 MPa) and 4000 ksi (28 GPa) for the grouting materials, and 6000 psi (41 MPa) and 4400 ksi (30 GPa) for the overlay. Poisson's ratio of 0.2 was assumed for the concrete and the grout. The steel was assumed to be an elastic-perfectly plastic material and identical in tension and compression. Poisson's ratio, yield strength (f_y), and E of 0.3, 60 ksi (420 MPa), and 29000 ksi (200 GPa) were used for the steel reinforcement, respectively. Fig. 8 shows the used stress-strain curves for the concrete and the reinforcing steel. The shear stud connectors were assumed to be an elastic-perfectly plastic material and identical in tension and compression. Poisson's ratio, f_y , and E elastic modulus of 0.3, 36 ksi (250 MPa), and 29000 ksi (200 GPa) were used for the steel beams, shear studs, and loading plates, respectively. The post-tensioning strands have f_y of 243 ksi (1700 MPa), an ultimate tensile strength of 270 ksi (1800 MPa), a cross-sectional area of 0.217 in.² (137 mm²), an E of 28000 ksi (193 GPa), and a relaxation of 2.5%. The post-tensioning bars have f_y of 121 ksi (835 MPa), an ultimate strength of 156 ksi (870 MPa), a cross-sectional area of 1.58 in.² (10.2 cm²), an E of 30550 ksi (210 GPa), and a relaxation of 3.1%.

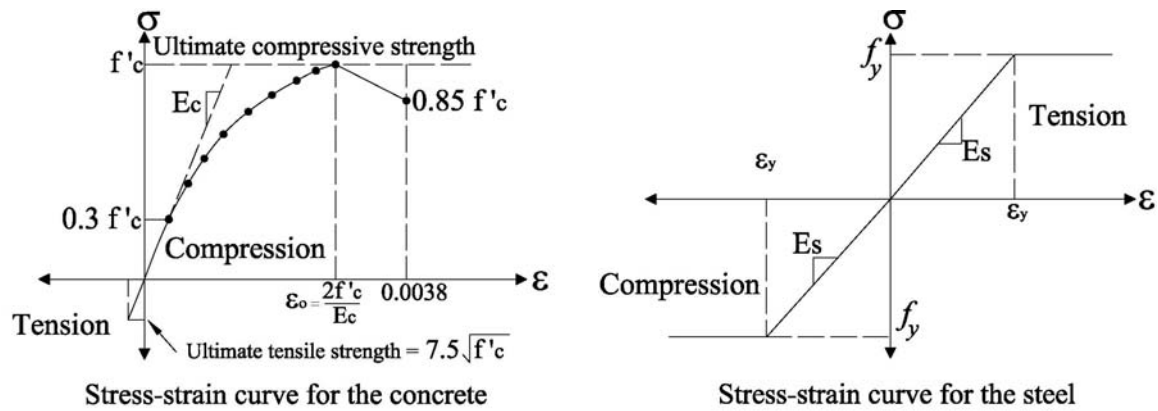


Fig. 8 The used stress-strain curves for the concrete and steel

MESHING AND ANALYSIS

Taking advantage of the symmetry in the prototype bridge system and the applied loading, half of the prototype bridge with proper boundary conditions was used in the FEA for the maximum negative and positive moment cases. This was carried out to reduce the computational time and computer disk space requirements. A convergence study was carried out to determine the appropriate mesh density. Fig. 9 shows the typical finite element meshing of half of the bridge with and without overlay. The total number of elements that were used in each FE model for half of the prototype bridge with the overlay was 145,000 elements. Perfect bond between the steel reinforcement and concrete as well as between the overlay and the deck were assumed. Close up views of the finite element meshing of the steel beams and the precast concrete deck along with the shear pockets and transverse joints are shown in Fig. 10.

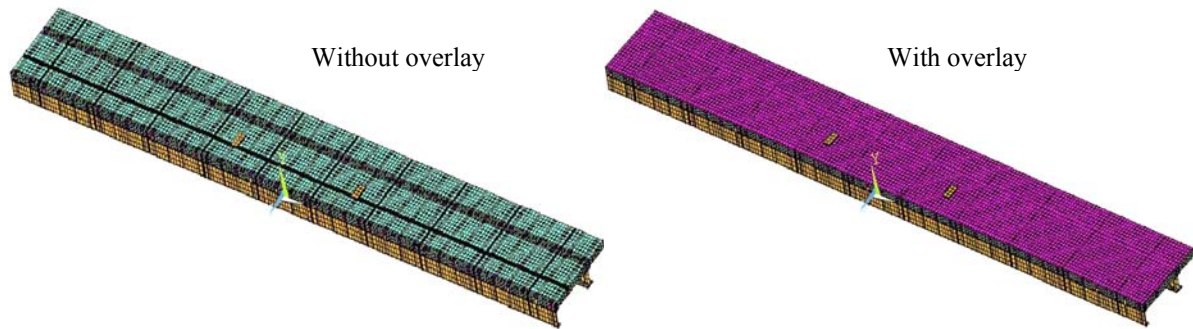


Fig. 9 Typical finite element meshing of half of the system with and without overlay

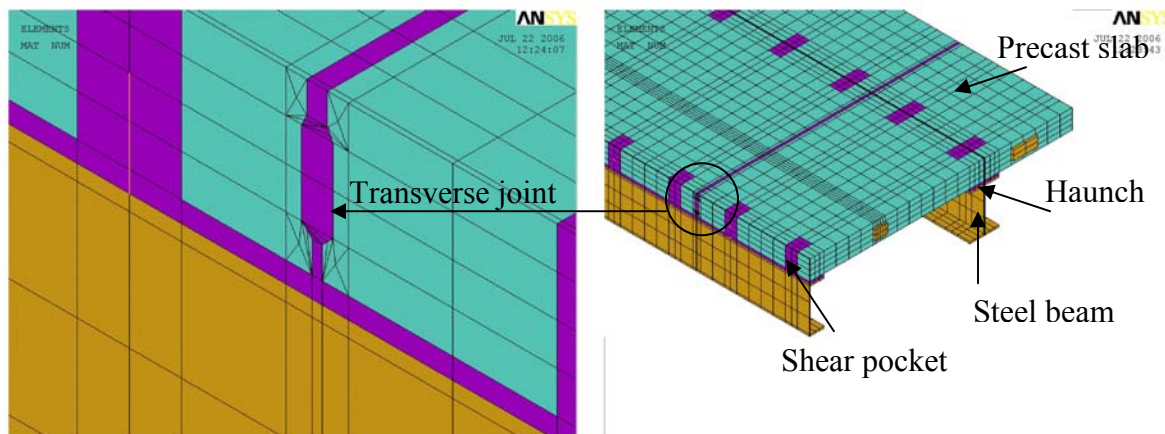


Fig. 10 Close up view of the finite element meshing of the steel beams and deck components

The total applied load was divided into a series of load increments and the Modified Newton–Raphson equilibrium iteration method was used in the analysis using a tolerance value of 0.001 to check the convergence at the end of each load increment. During concrete cracking and ultimate stage in which large numbers of cracks occur, smaller load increments were applied. Failure was identified for each model when the solution for a small load increment, 0.001 kip (0.0045 kN), was not converging. After completing each model, approximately 100 continuous hours were required to complete the run and to obtain the solution for each model.

FINITE ELEMENT ANALYSIS RESULTS

VALIDATION OF THE MODELS

In order to validate the finite element modeling, the load-deflection curves of the prototype bridge without overlay obtained from the FEA and the full-scale testing for the maximum negative and positive moment test cases were plotted as shown in Figs. 11 and 12. Inspection of Figs. 11 and 12 reveals that the FEA results are in good agreement with the full-scale test results in terms of stiffness, cracking load, ultimate load, and displacements. In

addition, the distributions of the cracks and strain values generated by the FEA were very close to the actual cracks that were observed during the full-scale testing. All these results assure that the used finite element models represent the actual system properties with high accuracy.

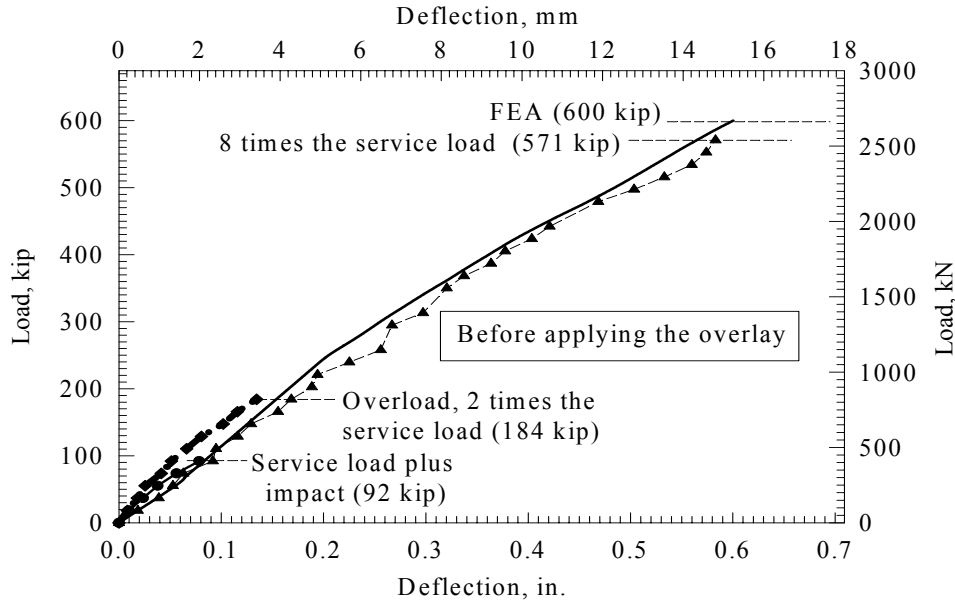


Fig. 11 Load-deflection curves for the maximum negative moment tests

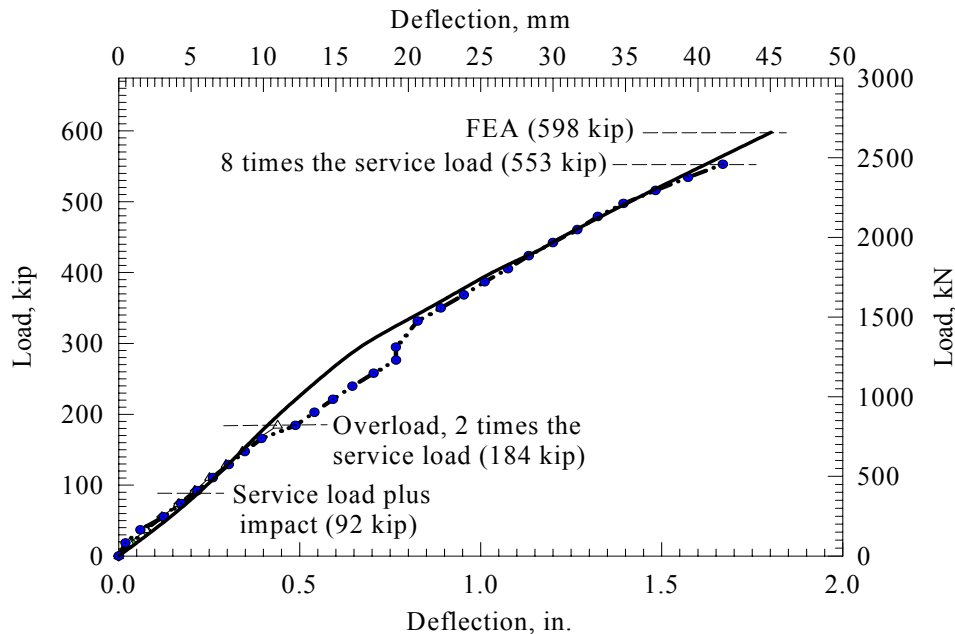


Fig. 12 Load-deflection curves for the maximum positive moment testing cases

PROTOTYPE BRIDGE WITHOUT OVERLAY

The FEA as well as the full-scale testing (Figs. 11 and 12) confirmed that the system is capable of withstanding and maintaining its integrity under a load representing about 8 times the simulated AASHTO truck service load without significant deterioration or reduction in its stiffness and ultimate strength capacity. The strain readings across the depth of the system (slab and beams) obtained from the full-scale testing and the FEA confirmed that full composite action between the precast concrete deck and the supporting system was achieved. In addition, no considerable slippage of the transverse joints was reported under all load cases.

PROTOTYPE WITH OVERLAY

The addition to the stiffness of the system by the bonded overlays can be visualized when comparing the experimental load-deflection responses for the system without overlay (Fig. 11) and the overlaid system (Fig. 13). The comparison shows that the stiffness of the overlaid system is about 10% higher, even though the LMC and MSC overlays were installed only on about 2/3 of the deck surface area. Also, the prototype bridge deck system was cracked and the steel stringers were yielded during the maximum negative moment and positive tests before installing the overlays. The epoxy overlays that were applied on 1/3 of the deck surface area are very thin; less than 1/2 in. (12 mm) thick; thus do not affect the stiffness of the system noticeably. If the LMC and MSC overlays were installed on the entire surface area of uncracked deck, it was anticipated that it would improve the stiffness of the system by more than 20%. This anticipation was verified by the FEA results as shown in the following paragraphs.

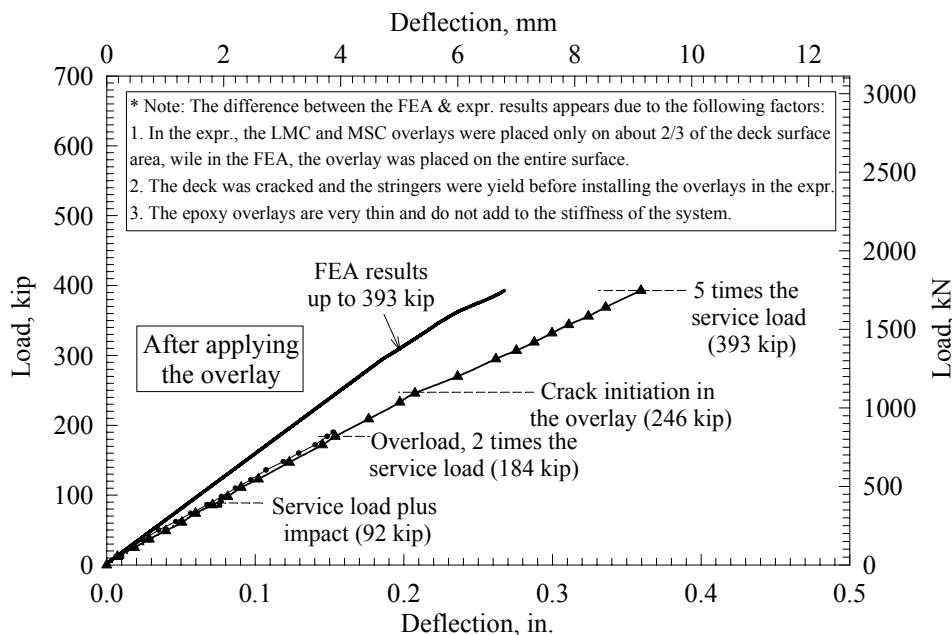


Fig. 13 Load-deflection curves of the overlaid system (maximum negative moment tests)

In all test cases, service load, overload, and 5 times the service load, the fatigue loading showed slight reduction in the stiffness of the system (Fig. 14) and minor deterioration in the overlays. Bond strength tests that were carried out at the maximum negative moment locations and around the loading points after each fatigue loading case, showed that no debonding was observed in the overlays. Detailed information about the effect of fatigue loading cycles on the structural behavior of the overlaid system as well as on the bond strengths of the overlays can be found in reference 17.

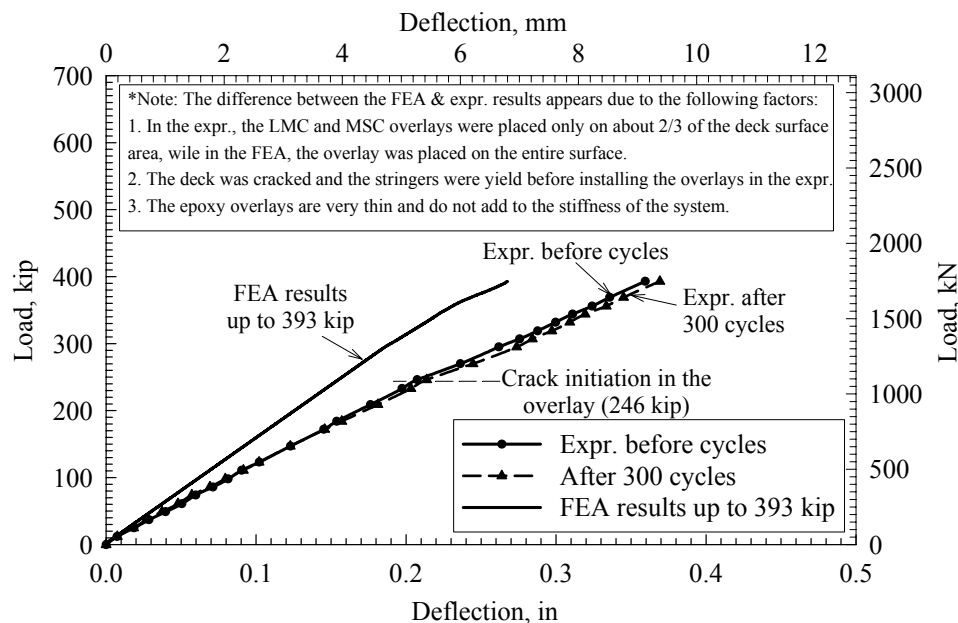


Fig. 14 Load-deflection curve of the overlaid system before and after fatigue loading

In the finite element modeling of the overlaid system, a 2¼ in.- (55 mm) thick concrete overlay having strength properties very close to the actual LMC and MSC properties was applied on the entire deck surface area. Full bond between the overlay and the deck system was assumed. This assumption was reasonable since in most of the conducted direct tensile bond strength tests, the deck-overlay bond was greater than the strength of the base concrete. In addition to that, the FEA was performed one more time for the overlaid system after introducing a crack above the central support (maximum negative moment region). The introduced crack was 1 in.- (25 mm) deep and continuous on the entire bridge deck width. Almost similar crack occurred in the system without overlay during the maximum negative moment full-scale testing. At the crack location, there was an LMC overlay with steel fibers and MSC overlay with synthetic fibers. The full-scale testing results showed that the crack arresting capability of the synthetic fibers was better than the steel fibers. This was attributed to the fact that the synthetic fibers have better uniform distribution throughout the overlay concrete than the steel fibers.

The load-deflection curves generated from the FEA for the system without overlay, with overlay, and with overlay on cracked deck are shown in Fig. 15. The curves clearly confirm that the overlay improved the stiffness of the system (about 23%), increased the cracking

load (about 40%), and increased the ultimate strength capacity of the system (about 10%). At any load value, for the precracking and the post-cracking behaviors, the deflection of the overlaid system was always less than the deflection of the system without overlay. For example at a load value of 500 kip (2225 kN), the deflection of the overlaid system was approximately 0.37 in. (9.5 mm), while the deflection of the system without overlay was approximately 0.53 in. (13.5 mm). The precracking behavior of the prototype bridge with a cracked deck was slight lower than the prototype bridge with uncracked deck. The post-cracking behavior was almost identical.

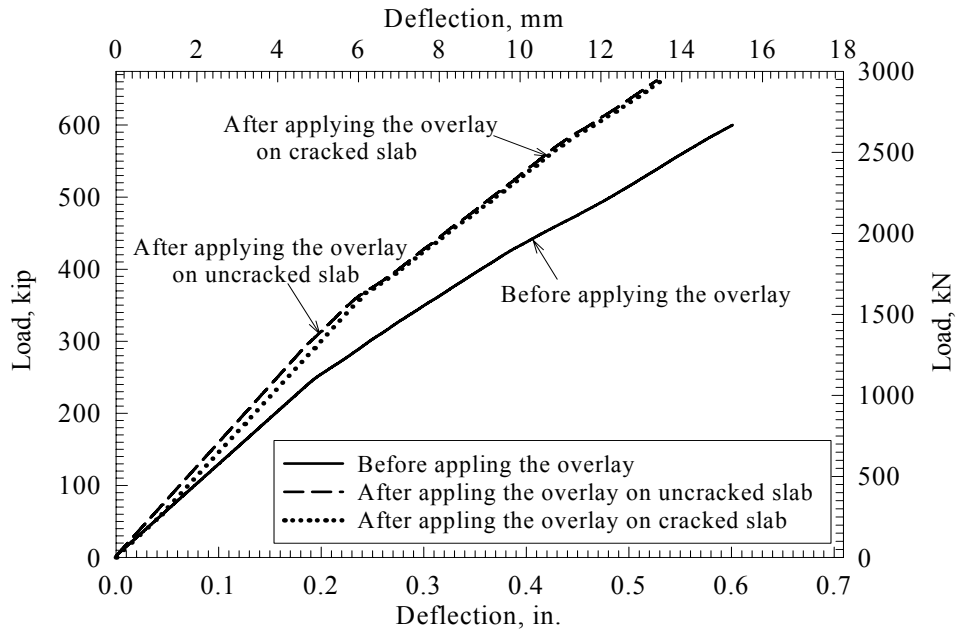


Fig. 15 Load-deflection curves generated from the FEA before and after the overlay

Typical deformed shapes and deflection values as well as stress and strain distributions generated from the FEA at ultimate for half of the prototype bridge before and after the overlay are shown in Figs. 16-20. These distributions demonstrate the critical locations for the system that experienced high deflection, strain, and/or stress values. In general, the distributions as well as the maximum values at the critical locations were in good agreement with the full-scale testing results. For example, Fig. 16 shows that the system without overlay has experienced an ultimate deflection of about 0.6 in. (15 mm) and the overlaid system has experienced lower ultimate deflection of about 0.53 in. (13 mm). These results are the ultimate deflections shown in Fig. 15.

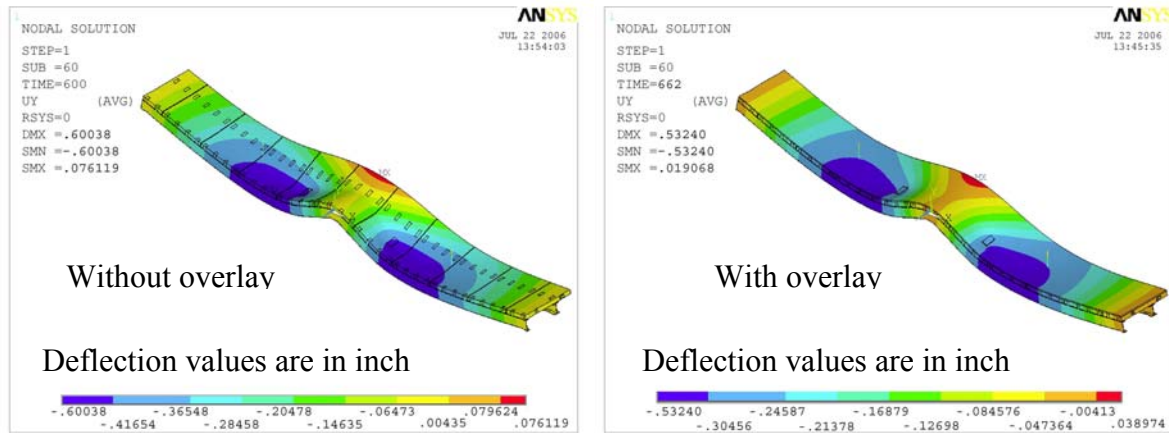


Fig. 16 Deformed shape before and after the overlay, values are in inch

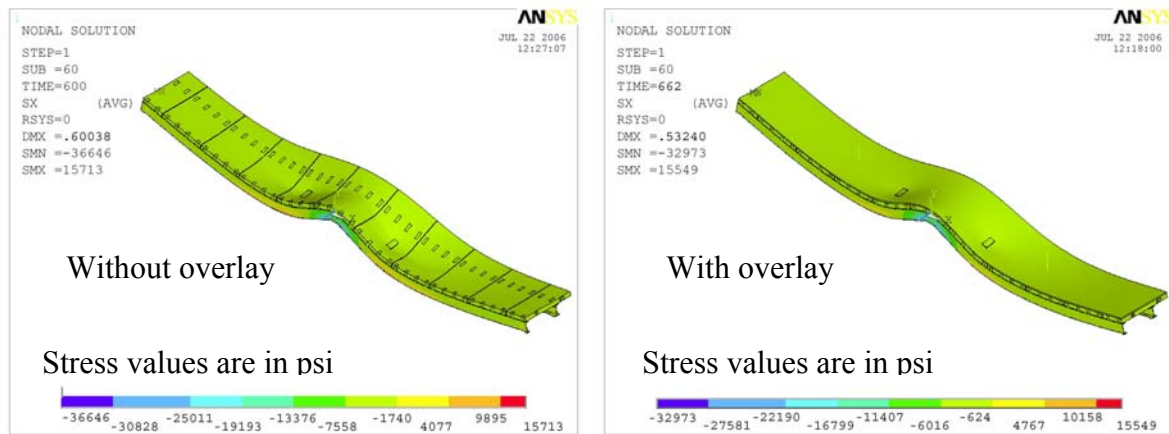


Fig. 17 Stress distributions before and after the overlay, values are in psi

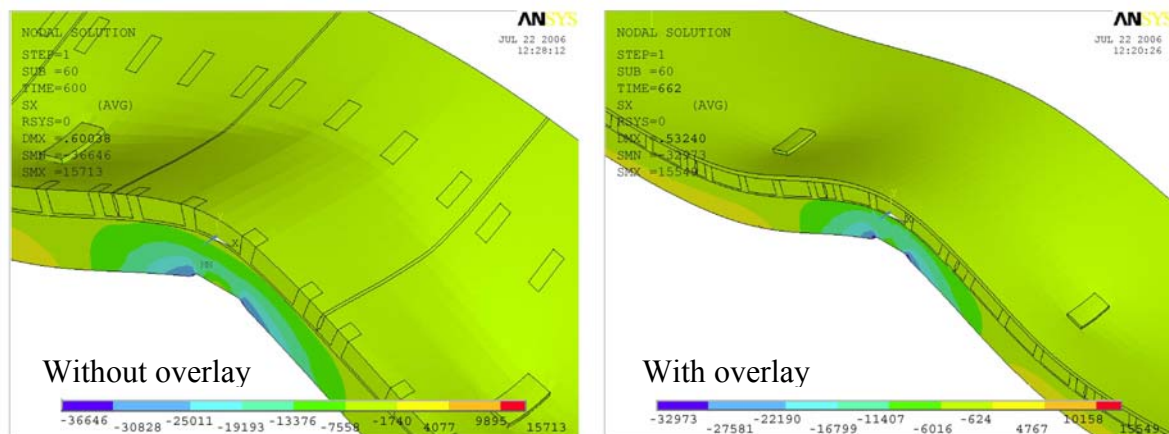


Fig. 18 Magnification of the stress distributions at the maximum negative moment region

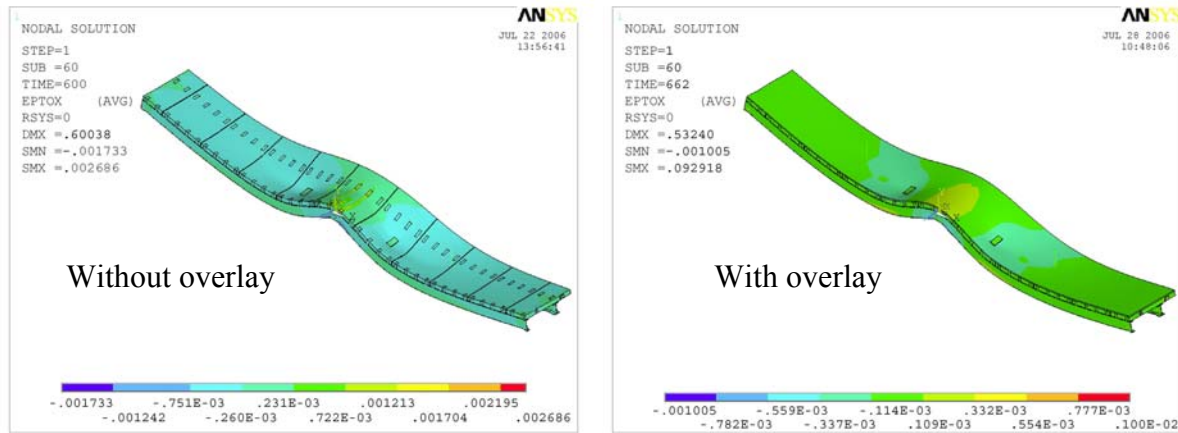


Fig. 19 Strain distributions before and after the overlay

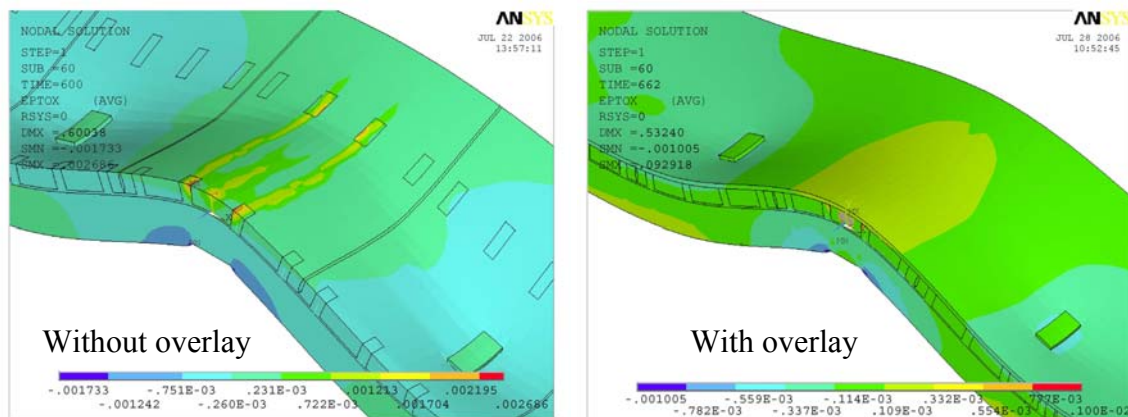


Fig. 20 Magnification of the strain distributions at the maximum negative moment region

LIVE LOAD-INDUCED BOND STRESSES

The induced shear and normal bond stresses between the overlay and the bridge deck at the maximum negative moment region (overlay in tension) were of particular interest. In order to avoid debonding of the overlay due to live loading, the overlay has to crack before the induced shear and normal stresses exceed the shear and direct tensile bond strengths of the overlay. The full-scale testing of the overlaid system and the followed direct tensile bond strength tests showed that the overlay cracked without showing any sign of debonding. Using the FEA results, the maximum induced shear and normal bond stresses at the maximum negative moment region were plotted versus the applied load as shown in Fig. 21. The stresses were generated for two situations; the overlay on uncracked deck and the overlay on a cracked deck.

For the overlay on uncracked deck, Fig. 21 shows that at a load value of 92 kip (410 kN), which simulates the AASHTO HS20 truck surface load plus 30% impact, the induced shear bond stress was about 180 psi (1.4 MPa) and the normal bond stress was about 35 psi (0.35 MPa). These results show that the induced bond stresses due to live loading themselves are

small and do not lead to delamination of the overlays since the experimental bond strength tests showed that the LMC and MSC overlays with and without fibers had direct tensile bond strengths greater than 450 psi (3.1 MPa). The shear bond strength of a bonded LMC or MSC overlay is at least 2 times its direct tensile bond strength, i.e. 900 psi (6.2 MPa), which is greater than the tensile strength of the overlay concrete (650 psi). However, there are some important factors that may play direct or indirect role in debonding of the overlays. Fatigue live loading leads to a reduction in the bond strength. In addition, after cracking of the overlay and the cracks reach the bond interface, the overlay delamination is expected to initiate at these locations due to the facts that the intensity of the induced stresses will be high around the cracks tips. The cracks will facilitate the intrusion of the deicing salts to the interface and introduce damage to the bond strength. For the overlay on uncracked deck, value of 92 kip (410 kN), the induced shear bond stress at the crack tip was about 300 psi (1.4 MPa) and the normal bond stress was about 80 psi (0.35 MPa). Although, these values still lower than the bond strength of the overlay, but they are almost double the bond stresses in the case of uncracked deck. These factors in conjunction with the induced bond stresses by thermal and shrinkage stresses as well as the fatigue live loading are the direct reasons for the delamination of the overlay.

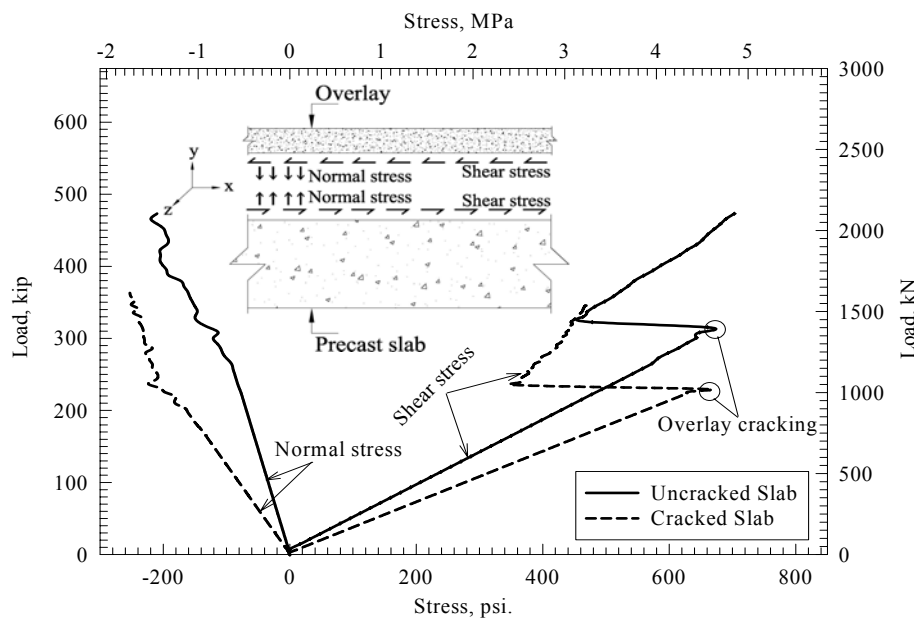


Fig. 21 Shear and normal bond stresses versus the applied load

CONCLUSIONS

Based on the experimental test results and the FEA, the following conclusions can be drawn:

1. Bonded concrete LMC and MSC overlays with direct tensile bond strengths greater than 450 psi (3.1 MPa) act structurally with concrete decks thus, improve the stiffness of the bridge and its ultimate strength capacity.
2. High bond strengths for the LMC and MSC overlays can be achieved using well-proportioned concrete mixtures in conjunction with acceptable construction practices, especially, the deck surface preparation, overlay placement, finishing, and curing.
3. Addition of discontinuous fibers to MSC or LMC overlay leads to a tough overlay with substantial crack arresting characteristics. The overlay with synthetic fibers showed better crack arresting mechanism than the overlay with steel fibers. Neither the synthetic nor steel fibers noticeably reduced bond strengths of the LMC and MSC overlays.
4. The nonlinear FEA were in good agreement with the experimental test results. If properly crafted and validated with respect to real experimental test results, the FEA provides substantial savings in the cost, time, effort, and allows for studying the influence of various critical and complex factors on the performance of the system.
5. For the overlay on a cracked deck, the FEA showed that the live load-induced normal and shear bond stresses at the crack tip location were almost double the corresponding normal and shear bond stresses for the overlay on an uncracked deck.

ACKNOWLEDGEMENT

This study was funded by a contract awarded to the University of Illinois at Chicago (UIC) by the Modjeski and Masters, Inc./IDOT. Their financial support is gratefully acknowledged. Thanks are due to Jeff Krozel, Prairie Materials, for supplying the MSC. Thanks are also due to Gary Vandenbroucke, Henry Frerk Sons, Inc., for supplying the LMC.

REFERENCES

1. Maher, T.K., "Rapid Replacement of Bridge Decks," Final Report, 12-41, National Cooperative Highway Research Program, Transportation Research Board, July 1997.
2. Issa, M.A., Yousif, A.A., Issa, M.A., Kaspar, I.I., and Khayyat, S.Y., "Analysis of Full Depth Precast Concrete Bridge Deck Panels," *PCI Journal*, Vol. 43, No. 1, January-February 1998, pp. 74-85.
3. Issa, M.A., Yousif, A.A., and Issa, M.A., "Experimental Behavior of Full-Depth Precast Concrete Panels for Bridge Rehabilitation," *ACI Structural Journal*, Vol. 97, No. 3, May-June 2000, pp. 397-407.
4. Issa, M.A., Anderson, R., Domagalski, T., and Khayyat, S., "Design Considerations of Full Depth Precast/Prestressed Concrete Bridge Deck Panels," Proceedings of the 1st

- annual Concrete Bridge Conference sponsored by FHWA and NCBC, and organized by PCI, October 2002, 20 p.
5. Issa, M.A., Idriss, A.T., Kaspar, I.I., and Khayyat, S.Y., "Full Depth Precast and Precast, Prestressed Concrete Bridge Deck Panels," *PCI Journal*, Vol. 40, No. 1, January-February 1995a, pp. 59-80.
 6. Issa, M.A., Yousif, A.A., and Issa, M.A., "Construction Procedures for Rapid Replacement of Deteriorated Bridge Decks," *Concrete International*, Vol. 17, No. 2, Feb. 1995b, pp. 49-52.
 7. Issa, M.A., Yousif, A.A., and Issa, M.A., "Structural Behavior of Full Depth Precast Prestressed Concrete Bridge Deck Replacement," Final Report, Illinois Department of Transportation, October 1995c.
 8. Issa, M.A., Yousif, A.A., Issa, M.A., Kaspar, I.I., and Khayyat, S.Y., "Field Performance of Full Depth Precast Panels in Bridge Deck Reconstruction," *PCI Journal*, Vol. 40, No. 3, May-June 1995d, pp. 82-108.
 9. Issa, M.M., Salas, J.S., Shabila, H.I., and Alrousan, R.Z., "Composite Behavior of Prefabricated Full-Depth Precast Concrete Panels Installed on Precast Prestressed Girders," *PCI Journal*, September/October 2006.
 10. Issa, M.A., Anderson, R., Domagalski, T., Asfour, S., and Islam, M.S., "Full-Scale Testing of Prefabricated Full-Depth Precast Concrete Bridge Deck Panel System," *ACI Structural Journal*, Accepted for Publication, 2006.
 11. Sprinkel, M.M. and Moen, C., "Evaluation of the Installation and Initial Condition of Latex Modified and Silica Fume Modified Concrete Overlays Placed on Six Bridges in Virginia," VTRC 99-IR2, Charlottesville, 1999.
 12. Sprinkel, M.M., "Delamination of the overlays on the Creve Coeur Lake Memorial Park Bridge," Virginia Highway & Transportation Research Council, Charlottesville, 2003.
 13. Issa, M.A., "Evaluation and Recommendation of Overlay Materials for the New Mississippi River Bridge," Illinois Department Of Transportation (IDOT), Final Report, Submitted, 2004, 200 p.
 14. AASHTO, Standard Specifications for Highway Bridges, 16th edition, American Association of State Highway and Transportation Officials, Washington, D.C., 1996.
 15. AASHTO, LRFD Bridge Design Specifications, American Association of State Highway and Transportation Officials, Washington, D.C., 1994.
 16. ANSYS, ANSYS User's Manual Revision 9.0, ANSYS, Inc.
 17. Issa, M.M., Alhassan M.A., and Shabila, H.I., "Low Cycle Fatigue Testing of HPC Bonded Overlay-Bridge Deck Slab Systems," *ASCE Journal of Bridge Engineering*, Accepted for publication, 2006.